

THE PRODUCTION AND SEPARATION
OF
MAGNESIUM IONS

Thesis

by

John C. Evvard

In partial fulfillment of the requirements
for the degree of Doctor of Philosophy

California Institute of Technology

Pasadena, California

1943

TABLE OF CONTENTS

	Page
I	Introduction 1
II	The Principal of Operation of the Ion Source
	A. Original Form. 5
	B. The Finkelstein Modification 5
III	Construction Details
	A. The Source of Magnesium Vapor. 8
	B. The Container for the Magnesium. 8
	C. Construction of the Copper Plate 10
IV	Source I
	A. Further Construction Details 12
	B. The Wiring Diagram 18
	C. Experimental Results 20
	D. The Problem of Resolution 22
V	Source II. 32
VI	Theoretical Resolution 42
VII	Field Penetration. 48
VIII	Bibliography 53

INTRODUCTION

Since the definite proof of the existence of isotopes, in 1912, the methods of separation of the various mass units of a given element are becoming more and more important. The use of isotopic tracers in chemistry, the need for pure samples for nuclear reaction experiments, the enhancement of nuclear spin data, etc, may be mentioned as some of the more common uses of pure isotopic samples. For this reason, many ingenious separation schemes, some good, some bad, have been described in the literature. A summary of these appears in Aston's book MASS SPECTRA AND ISOTOPES. A more critical analysis of the advantages and disadvantages of the best of these is covered by ISOTOPENTRENNUNG by W. Walker published in ERGEBNISSE DER EXAKTEN NATURWISSENSCHAFTEN XVIII BAND 1939. These can be classed in two groups: (1) those that depend upon the rates of migrations of neutral atoms, and (2) those that depend upon the accelerations of ionized atoms.

The more common of these methods that fall in the first group are:

1. Separation through diffusion. (Hertz)
2. Separation through fractional distillation.
3. Separation through thermal diffusion.
(Clusius Dickel)

4. Separation by means of a centrifuge.
5. Separation by gravitation. (Sometimes called pressure diffusion).

Those that fall in the second classification are:

1. Separation by mass-ray analysis.
2. Separation by electrolysis.
3. Separation by chemical and photo-chemical action.

Of the various methods listed above, by far the most complete separation so far achieved has been accomplished by means of the mass spectrometer. While practically 100% separation has been achieved with its use, the size of the sample that can be collected is necessarily limited by the strength and durability of the ion source. To make the strength of the ion source greater it is desirable to use an extended rather than a point source. An extended source increases the ion current to the collector because: (1) there is a larger ion emitting surface, and (2) the mutual space charge repulsion per unit ion current is less in an extended ion beam than in a confined ion beam.

For this reason Dr. William R. Smythe designed and constructed a mass spectrometer* at the California Institute of Technology which focused ions

* Type I. Note notation of Lynn H. Rumbaugh, Ph.D. thesis, 1932.

of the same mass and charge from a line source to a point collector after passing through the magnetic field. This was successfully used by Dr. Smythe during 1924 and 1925, and later by other men at the laboratory. An improved Type II instrument was designed and constructed by Dr. Smythe and Lynn H. Rumbaugh between 1929 and 1932. From 1932 to 1934 Dr. George Steward West designed and built ion sources for the Type II lens. These were of the Kunsman catalyst variety. Dr. Arthur Hemmendinger took over the work of Dr. West in 1934 and put the whole instrument and ion source in satisfactory operation. With it he was able to collect samples containing several milligrams of potassium and rubidium and to settle successfully the long disputed controversy concerning the radio-active isotope of potassium. The situation after the completion of the work by Dr. Hemmendinger was that the application of the Type II spectrometer was limited by the lack of new ion sources. For this reason, Dr. Smythe and the author decided to build an ion source which depended upon electron bombardment to ionize the atoms. It was hoped that this source could be applied to certain vaporizable metals.

Incorporated in this source was the Finklestein improvement to increase greatly ion current. This thesis deals with the problems and their solutions which were met in the production of a high intensity positive ion source of magnesium ions.

THE PRINCIPAL OF OPERATION OF THE ION SOURCE

A hot filament A (Figure 1) is used to produce electrons. These electrons are accelerated toward the plate B which is at a positive potential with respect to the filament. The gas to be ionized is injected into the chamber C through the inlet tubes D. Occasionally an electron will give up its energy to a neutral atom, thereby producing an ion. This positive ion is then accelerated toward the negative filament which is wound in such a manner that most of the ions will pass right through it into the region of an accelerator plate G. It is seen that with such a source: (1) an electron is lost as far as the source is concerned after it has crossed the region C once without producing an ion. (2) Only a very few of those electrons which are emitted will produce ions. (3) To get appreciable ionization many electrons must be emitted by the filament.

The Finkelstein Modification

A schematic diagram of the Finkelstein modification is shown in Figure 2. We have seen above that an electron was captured after crossing the region C. However, if we were to put in an electrode F set at the same potential as the filament A, the

Schematic Sources

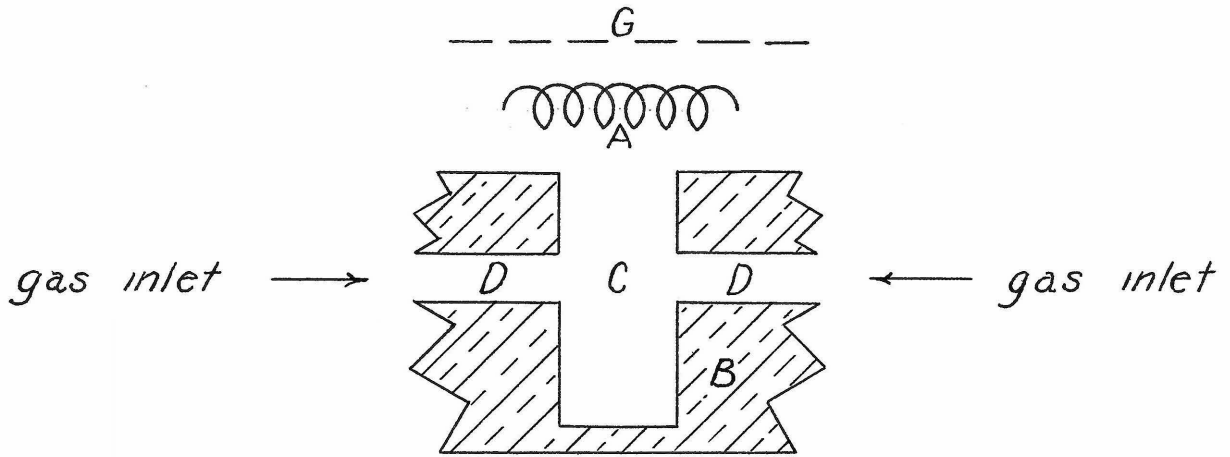


Figure 1

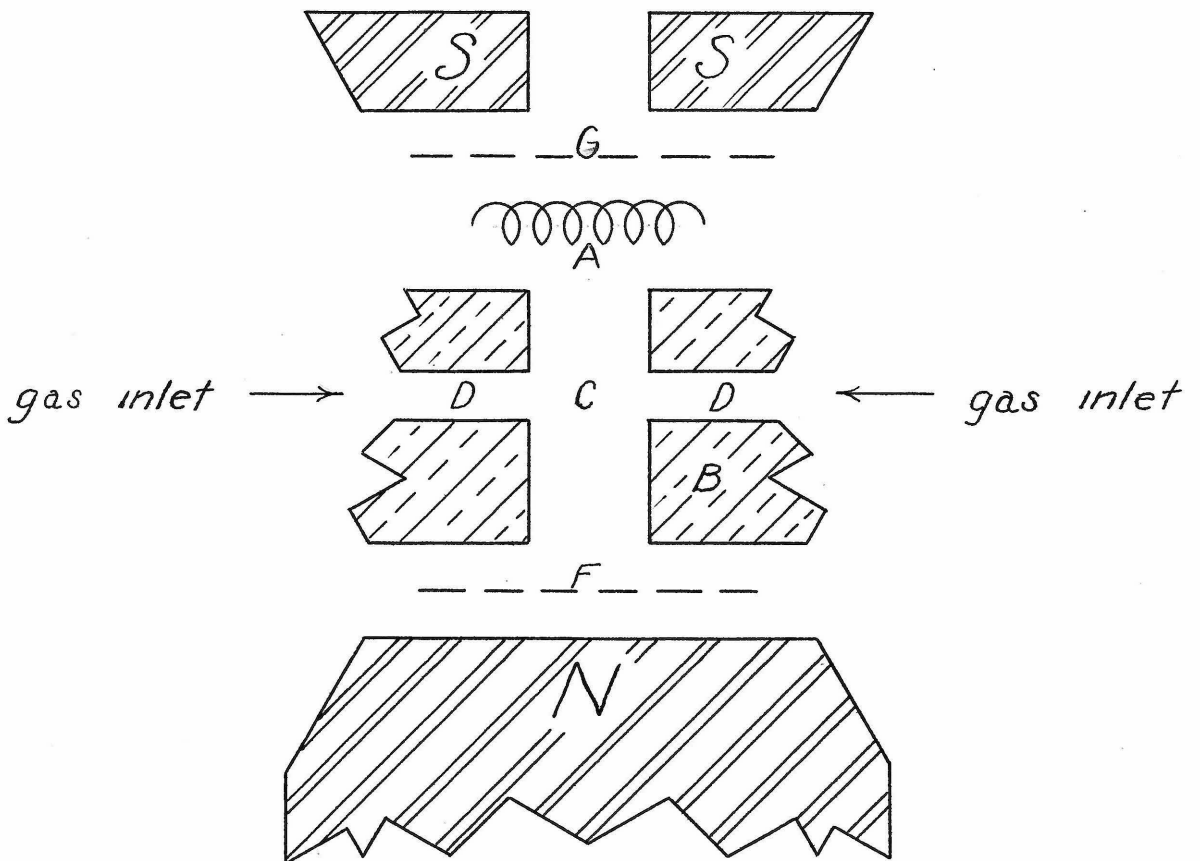


Figure 2

electron would come to a halt just before striking F and then accelerate back toward the region C. Furthermore, if a magnetic field is placed parallel to the axis A-C, an electron which tends to diverge toward the plate B will be kept close to the axis and hence will be bounced back and forth between A and F until it finally ionizes an atom or is captured.

It is seen that with this arrangement of the source, there is a saddle point in the region C. If a positive ion is formed above the saddle point, the ion will go up toward the filament A. If it is formed below the saddle point, it will go down toward F. However, only the ions which are going a given direction can be utilized. Hence, it is seen that we have two alternatives. Type I: the source can be arranged so that the ions utilized will go toward the filament, and Type II: the source can be arranged so that the ions go away from the filament. Both of these arrangements have been constructed and used successfully to produce ions. The remainder of this paper will deal with the details of construction and operation of each.

THE SOURCE OF MAGNESIUM VAPOR

The source of the magnesium vapor was a cylindrical pipe of pure magnesium* about ten inches long, 5/8" O.D. and 5/16" I.D. This pipe (Figure 3) was heated by a furnace constructed by winding #24 nichrome wire between two concentric stupakoff tubes; .120" I.D., .196" O.D., and .278" O.D., respectively.

This furnace was then inserted into the magnesium pipe. Two such furnaces in series had a total resistance of 10 ohms and produced ample evaporation when they were run at from three to five amperes.

THE CONTAINER FOR THE MAGNESIUM

The hot magnesium alloys readily with many of the common metals below their natural melting temperatures. Furthermore, the resulting alloy decomposes readily in a vacuum. The problem was to find a material that would be non-magnetic and yet would have little tendency to alloy with magnesium. The first tubular container to be tried was made of brass. After several hours of operation, this tube had fairly large holes in the walls. Copper was then tried but found to be only slightly better. Stainless steel tubes (3/4" C.D., U.S. 18-8, permeability--1.003)

* Purchased from Dow Metal Co.

Furnace

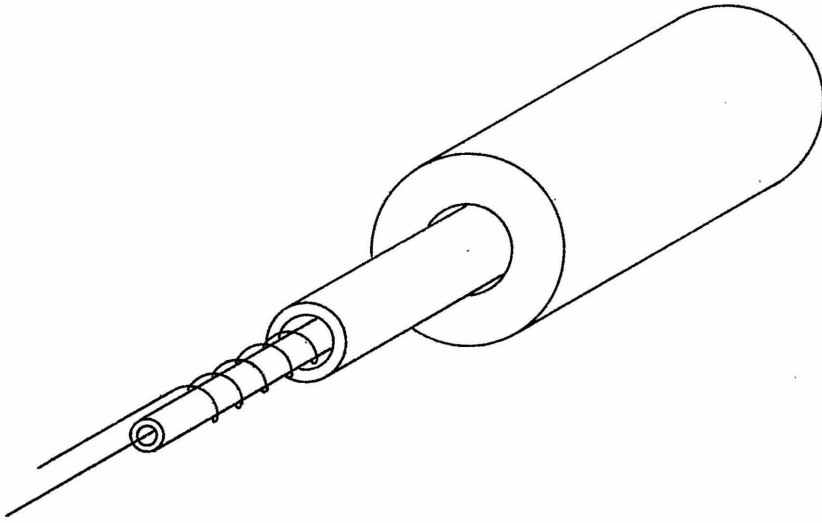


Figure 3

Plate

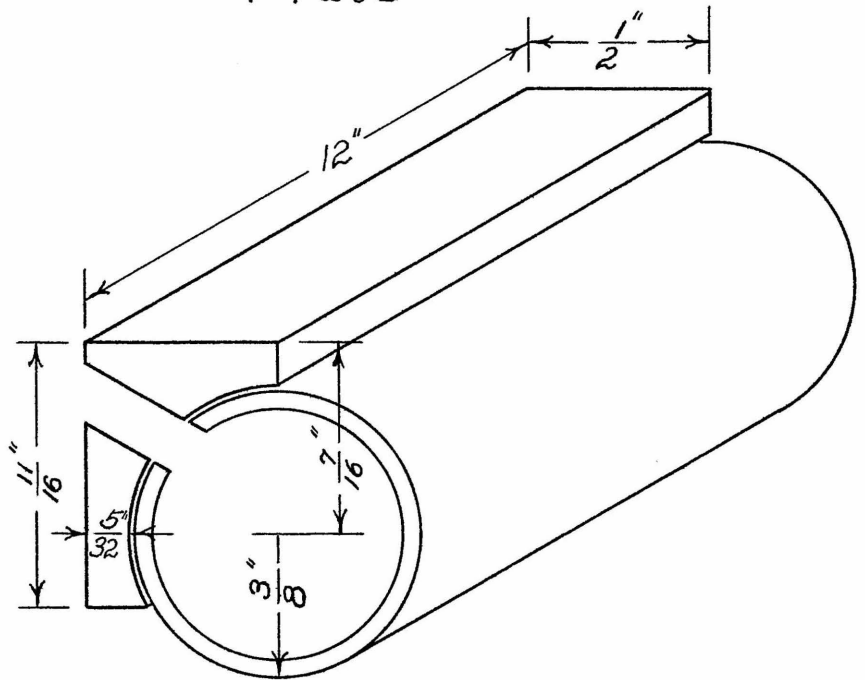


Figure 4

were then tried and found to be satisfactory. The steel tubes were then screwed to a milled copper block. Two such blocks screwed together formed the electron plate. Stainless steel is undoubtedly the best material to use for the plate, but copper is applicable in that it is a good conductor, does not contaminate the system extremely and has a thermal expansion that is not too different from that of stainless steel.

CONSTRUCTION OF THE COPPER PLATE

A piece of copper bar 12" by 1/2" by 11/16" was first milled to an approximately circular cut by means of a 3/4" end mill set at a very slight angle (Figure 4.) The stainless steel tube was then fastened to this by a single screw in the center and copper plugs on the ends of the tubing. These plugs were made to fit freely into the stainless steel tubes and then to flange out to a 3/4" diameter. The larger section was screwed securely to the copper, while the stainless steel tube fitted loosely over the smaller section. This allowed for the difference in thermal expansions of copper and stainless steel while the single screw in the center kept the tube from rotating. Having been screwed together, holes

were drilled with a #18 drill about $3/8$ " apart.
These were the gas inlets D of Figures 1 and 2.
Two such sections screwed together formed the chamber
C (Figure 5.)

SOURCE I

Figure 5 shows a scale drawing of Source I. The steel plate J was screwed to the copper plates B. The bouncer electrode F was made of iron and ran the length of the source. It was insulated from the copper plates by means of small pieces of glass K cut from thin spectroscopic plates. The magnetic pole pieces, N and S, furnished the field which kept the electrons on the axis. The tantalum filaments, A*, were supported to the iron pole pieces every $2\frac{1}{2}$ inches. If fewer supports were used, the interaction of the alternating heating current with the magnetic field caused the filaments to vibrate badly. Oxide coated filaments were tried successfully in a previous trial source of smaller dimensions. However, it was thought that due to the long length of the present source, these would prove unsatisfactory**.

Calculations showed that some mechanism is

* Strip tantalum filaments .005" x .085" x 10" purchased from the Fansteel Corporation were used. These had extremely constant cross-sections (as is desirable for long life and uniform emission).

** Thermal expansion of the filaments plus excessive vibration would probably destroy the oxide coating. It was found empirically that filaments or electrodes arranged perpendicular to, rather than parallel to, the source tended to destroy the resolution.

Source 1

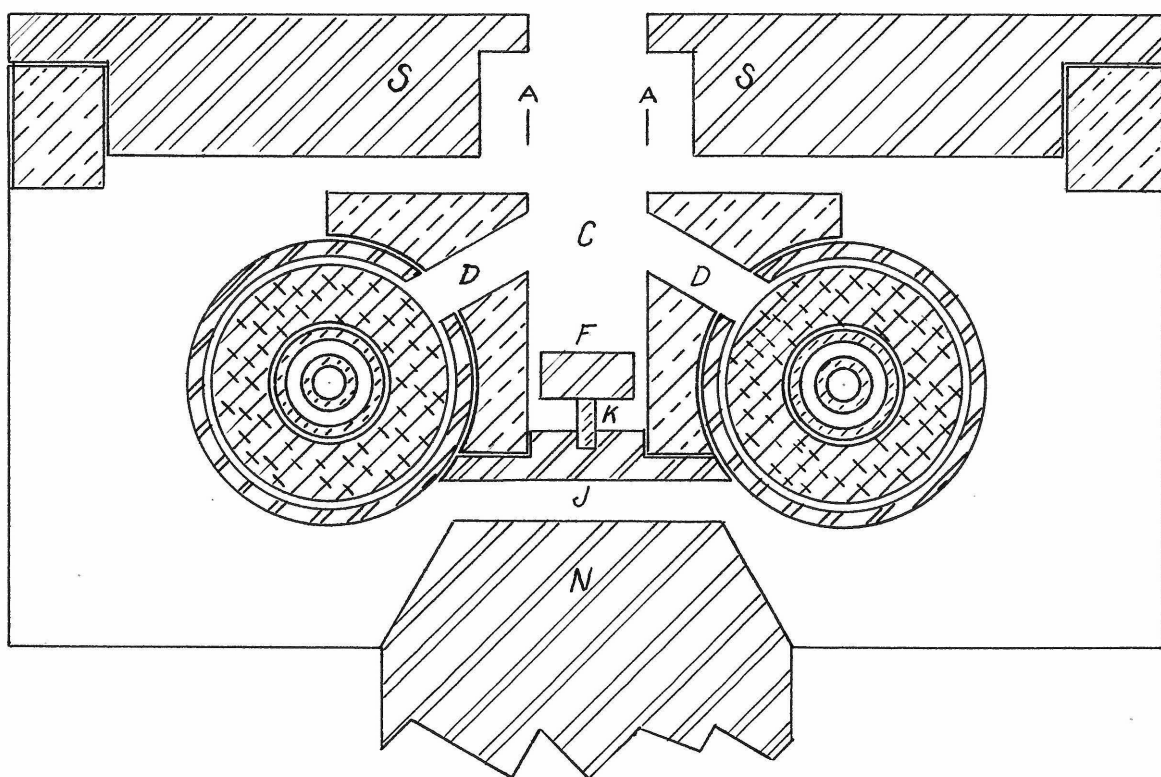


Figure 5

necessary to compensate for the thermal expansion of the filaments. The mechanism which proved satisfactory consisted of an $1/8$ " thick wheel mounted on a bearing. The filament and a spring actuated lever were fastened to the periphery of this disc, Figure 6. Due to the large currents that the filaments carried (in excess of 20 amps apiece) it was necessary to ground the wheels to the pole piece by means of an auxiliary wire rather than to depend upon the bearing surface for contact. The source block was used as one of the filament leads*. The other end of the two parallel filaments were spot-welded to a $1/8$ " thick nickel plate, cut to the width of the spacing between the filaments. This could be insulated from the supporting plate by a small soapstone insulator or by an arrangement similar to that shown in Figure 8c. The nickel plate, e, was held solidly to the supporting plate by the screw, a, which was insulated by the stupakoff tubing, b, and mica washers, d. This method gave no trouble.

The first auxiliary filament supports to be tried were made of sheet mica. These proved to be unsatisfactory because, apparently, there was a chemical reaction between the hot filaments and the mica,

* The two filaments were operated in parallel.

Filament Take-up

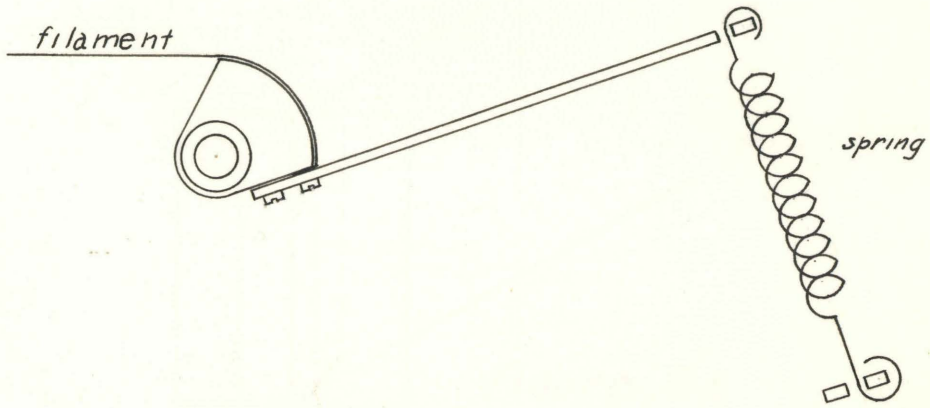


Figure 6



Figure 7

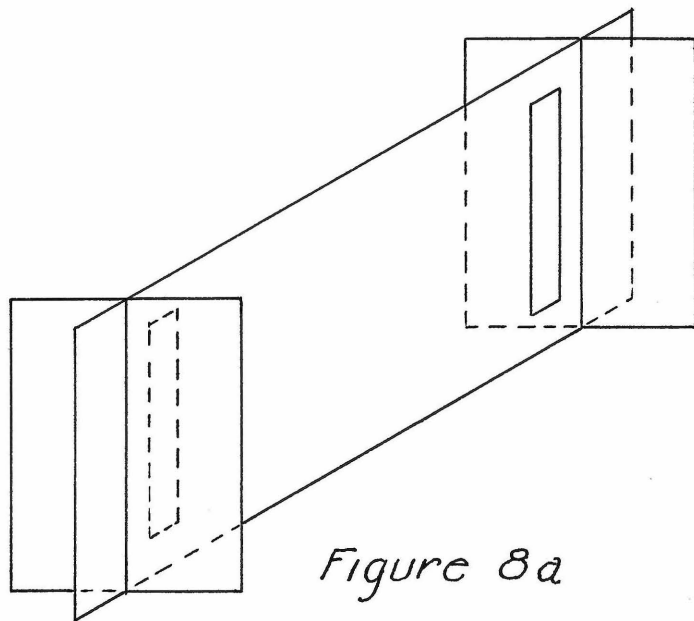


Figure 8a

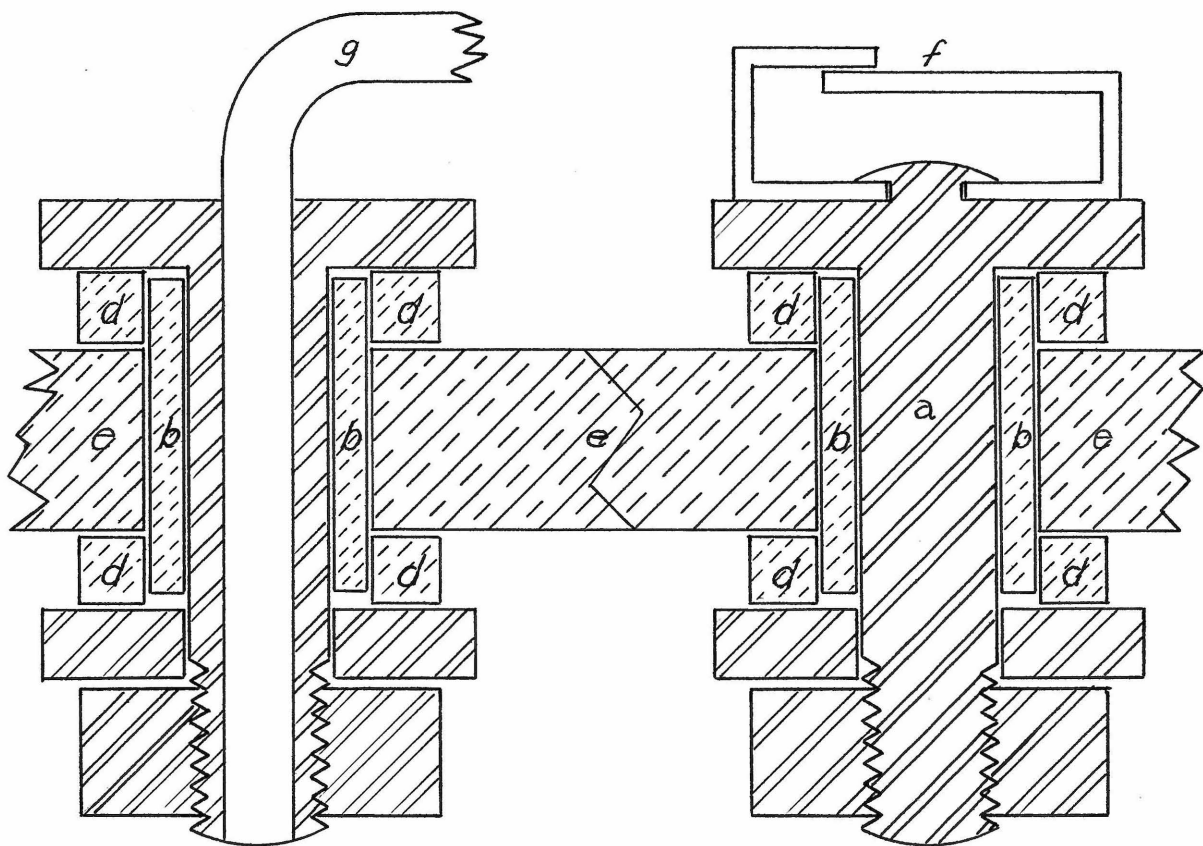


Figure 8b

Figure 8c

Figure 7. The second supports tried were made of molybdenum sheets .002" thick, Figure 8a. These were held in place by mica lined slots in the iron at the position of the mica supports seen in Figure 7. While they served their function of supporting the filaments, they destroyed the resolution (to be explained later.) The next support that was tried, Figure 8b, consisted of a tungsten wire bent to shape and set in a screw head drilled lengthwise. The wire was clamped by small steel pins wedged into the hole in the screw. These supports proved to be satisfactory both from the standpoint of resolution and support. Occasionally, the steel pins would loosen up; this suggested that as an improvement the tungsten could be welded to nickel screws. The final filament supports that were used, Figure 8c, had molybdenum strips riveted to the screw head, a.

THE WIRING DIAGRAM

A schematic arrangement of the wiring diagram is shown in Figure 9. The plate B was connected to the positive terminals of a 6000 volt and a 150 volt source*. The negative side of the 6000 volt line was connected to the accelerator plate G and to the case of the spectrograph. The negative terminal of the 150 volt generator was connected to the source block to which one end of the filament was attached. The filament current was furnished by an insulation transformer controlled by means of a variable resistance in the primary**. A similar arrangement furnished current to the magnesium heaters. All connections could be altered at will as test conditions required.

It is interesting to note that when the electron-bouncing electrode F was left floating, it approximately assumed the same potential as the filament. When it reached that value, no more electrons could be captured by it. Thus, the potential of the bouncer electrode was automatically self balancing.

* The voltages were furnished by D.C., M.G. sets.

** The current in the secondary was of the order of 20 amps per filament while that of the primary was half as great.

Wiring Diagram

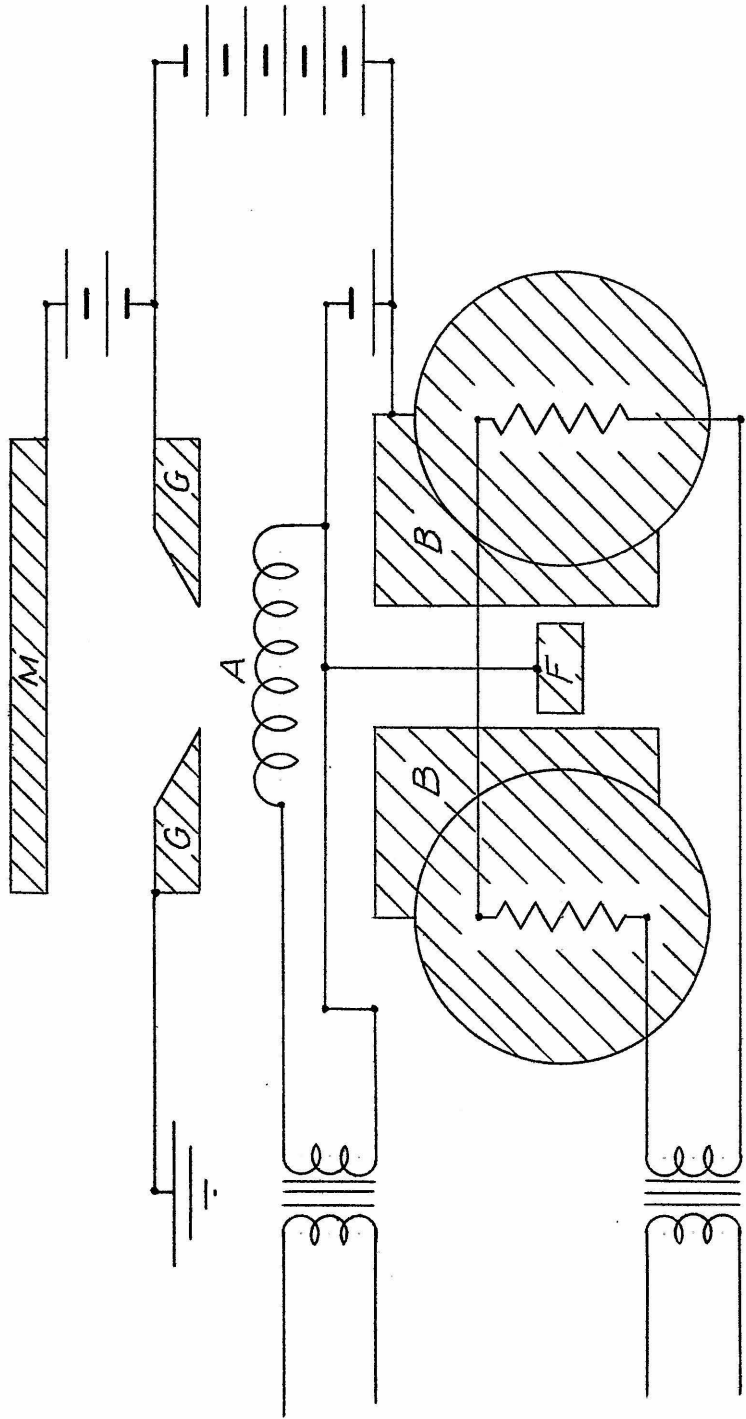


Figure 9

EXPERIMENTAL RESULTS OF SOURCE I

Preliminary trials

For the sake of convenience, let us adopt the following definitions:

Filament current--current used to heat the filaments.

Emission current--electron plus positive ion current to or from the filaments.

Plate voltage--potential difference between the plate, B, and filaments, A.

Accelerator voltage--potential difference between the plates, B, and the accelerator grid, G.

Bouncing field--magnetic field required to keep the electrons on the axis.

Heater current--current carried by the heaters of the magnesium.

For the purpose of measuring the positive ion current produced, the plate M (Figure 9) was installed and set at a potential of 45 volts above ground. This potential was adequate to prevent secondary emission. A positive ion current of 1.2 mils. was measured under the following conditions:

Electrode	Potential	
M	45 volts	Filament current 38 amps.
G	0 "	Heater current 3 amps.
A	650 "	Emission current 100 mils.
B	700 "	Vacuum 2×10^{-5} mm.
F	650 "	

The second test yielded a positive current of 1.4 mils under the following conditions:

Electrode	Potential	
M	45 volts	Filament current 30 amps.
G	0 "	Heater current 3 amps.
A	975 "	Emission current 100 mils.
B	1000 "	Vacuum 2×10^{-5} mm.
F	975 "	

It is interesting to note that the positive ion current was an extremely critical function of the plate voltage. Apparently, if the latter was too high, the electrons did not remain in the ionizing region long enough to produce ions. In each of the above cases, the plate voltage was set to give maximum positive ion current. These results were good enough to warrant a trial at separating magnesium isotopes in the mass spectrometer. This attempt brought on the problem of resolution.

THE PROBLEM OF RESOLUTION*

The mass spectrometer collecting slit width corresponding to one mass unit is approximately $W = 20/M$ where W is in centimeters. Thus, if a 2 mm. slit is used to collect mass 24, the slit integrates the current over .24 of a mass unit. This is small enough so that defects in resolution can not be attributed to the slit width.

For the sake of comparison, Figures 10 to 15 inclusive, have all been normalized. The following table gives a comparison of operating conditions**.

Fig.	Accelerator voltage (mass 24)	Vacuum at collector	Estimated vacuum at source	Bouncer at field
10	3430	10^{-5} mm.	good	on
11	3430	10^{-5} mm.	good	off
12	3440	10^{-5} mm.	good	off
13	3470	3×10^{-5} mm.	poor	off
14	3470	2×10^{-5} mm.	fair	off
15	3470	1.2×10^{-5} mm.	good	on?

Figure 10 shows the resolution curve of the source with the bouncing field at approximately 400 gaussess. The resolution is obviously not good. Figure 11 shows the observed curve under similar conditions except the magnetic field was turned off. Comparing

* See Rumbaugh, Ph.D. thesis for the theory of resolution.

** The collecting slit width was 2 mm.

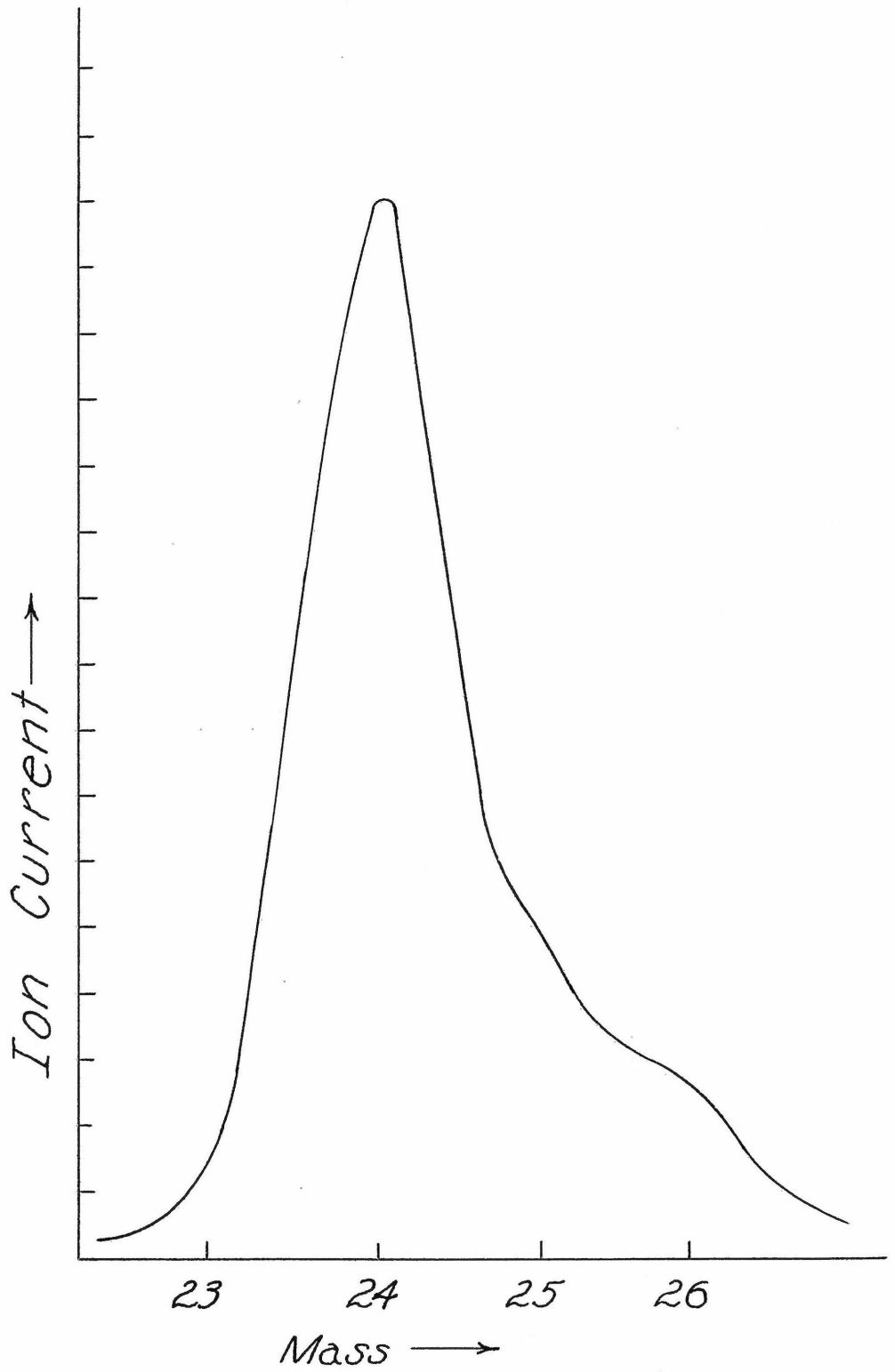


Figure 10

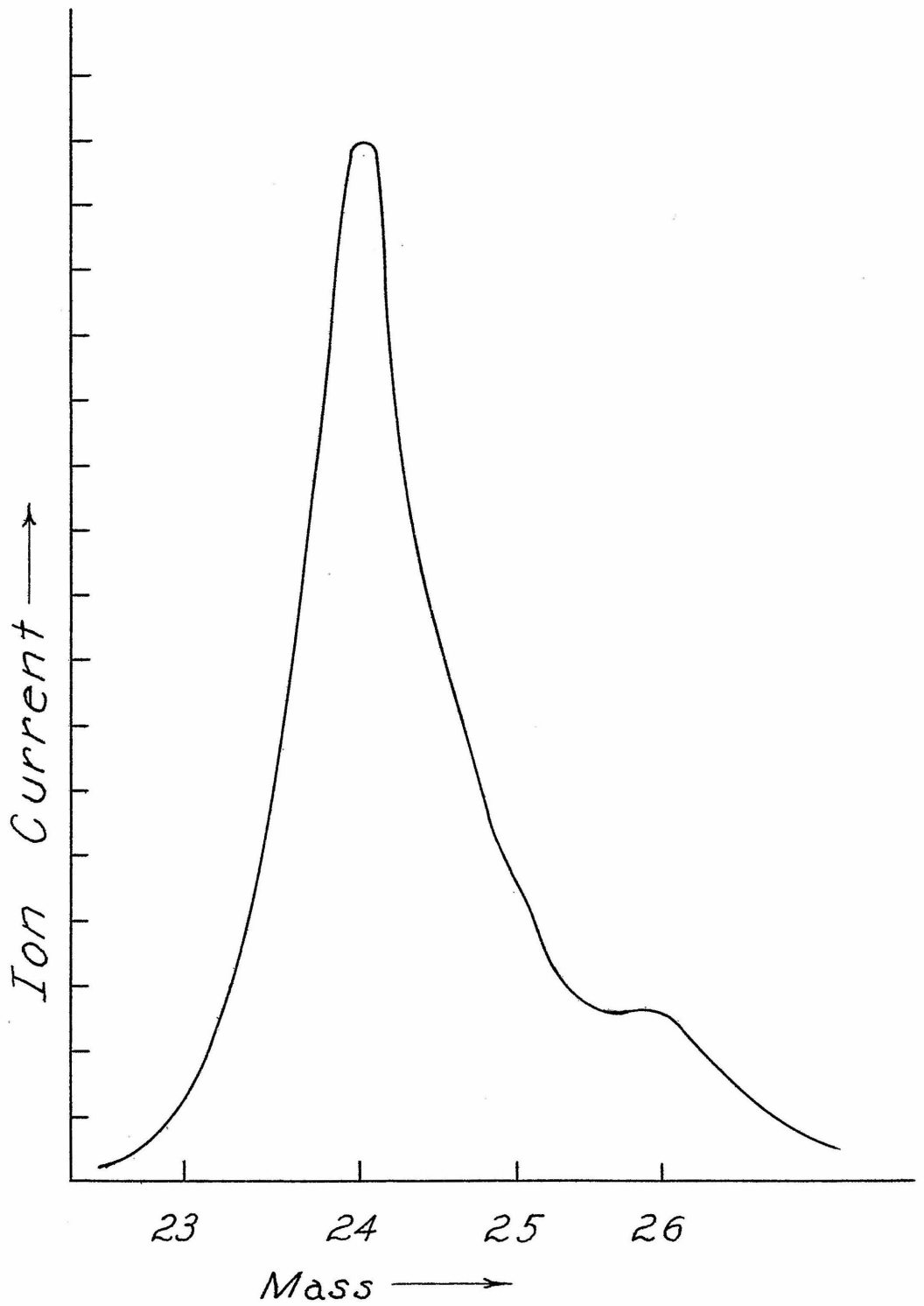


Figure 11

these two curves, it would appear that use of the magnetic bouncing field tended to destroy the resolution. This might be caused by the scattering effects due to increased space charge. The magnetic field made a difference of about 3 to 1 in the produced ions though less effect in collected ions.

The resolution is very sensitive to ion velocities parallel to the source. For this reason, it was thought that the lack of resolution might be caused by the alternating electric field produced by the IR drop along the filaments.* Figure 12 shows a curve traced while heating the filaments with direct current. Its shape is so singular that doubtful improvement resulted from this test.

Dr. Smythe suggested that the sharp edges of the molybdenum filament supports (Figures 7 and 8a) might be causing the scattering. To test this, the tungsten wire supports (Figure 8b) were installed. Figures 13, 14 and 15 certainly demonstrate that this was the chief factor in the poor resolution. Comparison of Figures 13 and 14 shows the effect of vacuum conditions on the resolution. Figure 15 shows a curve similar to Figure 14 except that the vacuum was

* This field amounted to about 2 volts per centimeter peak to peak.

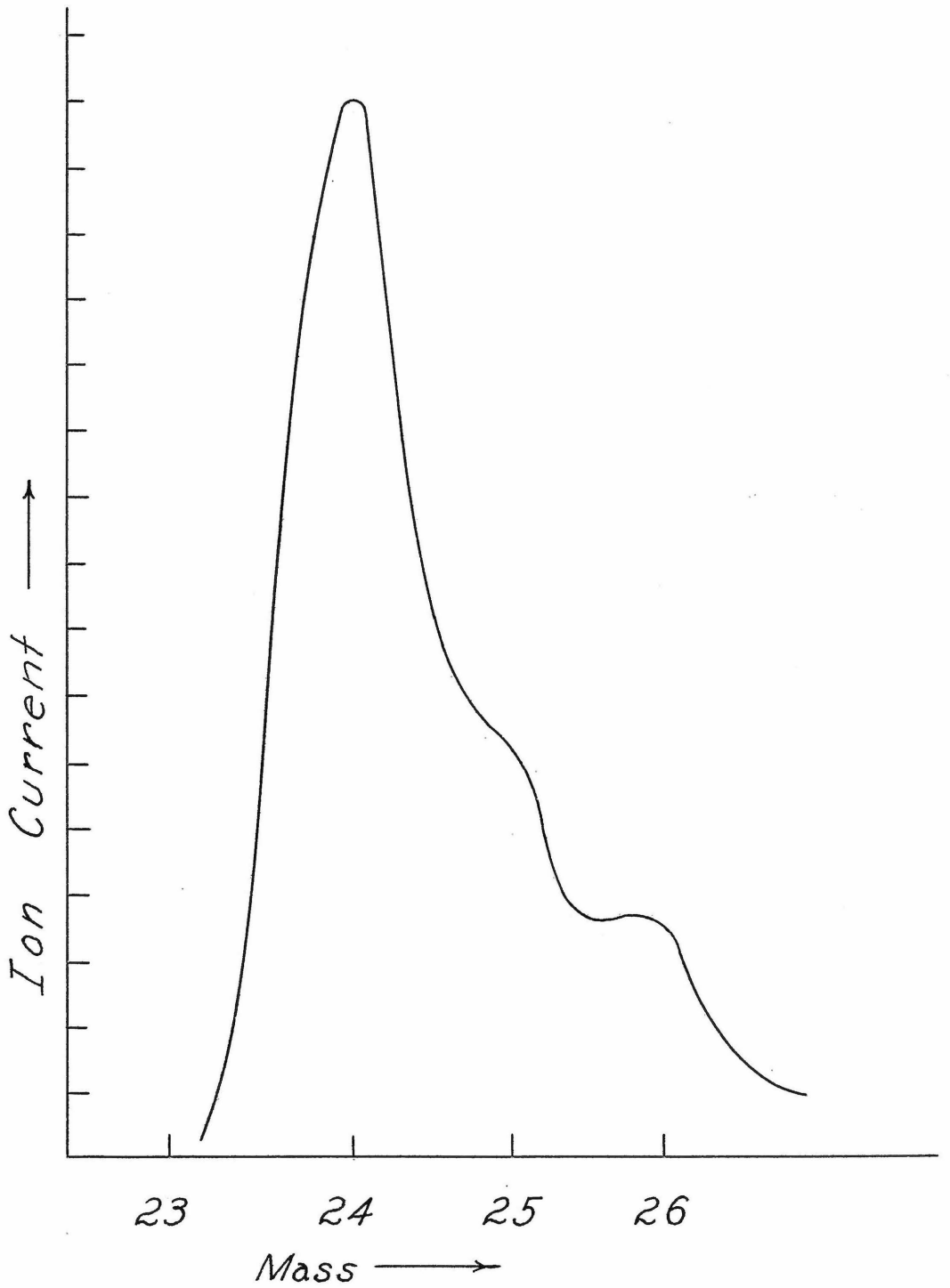


Figure 12

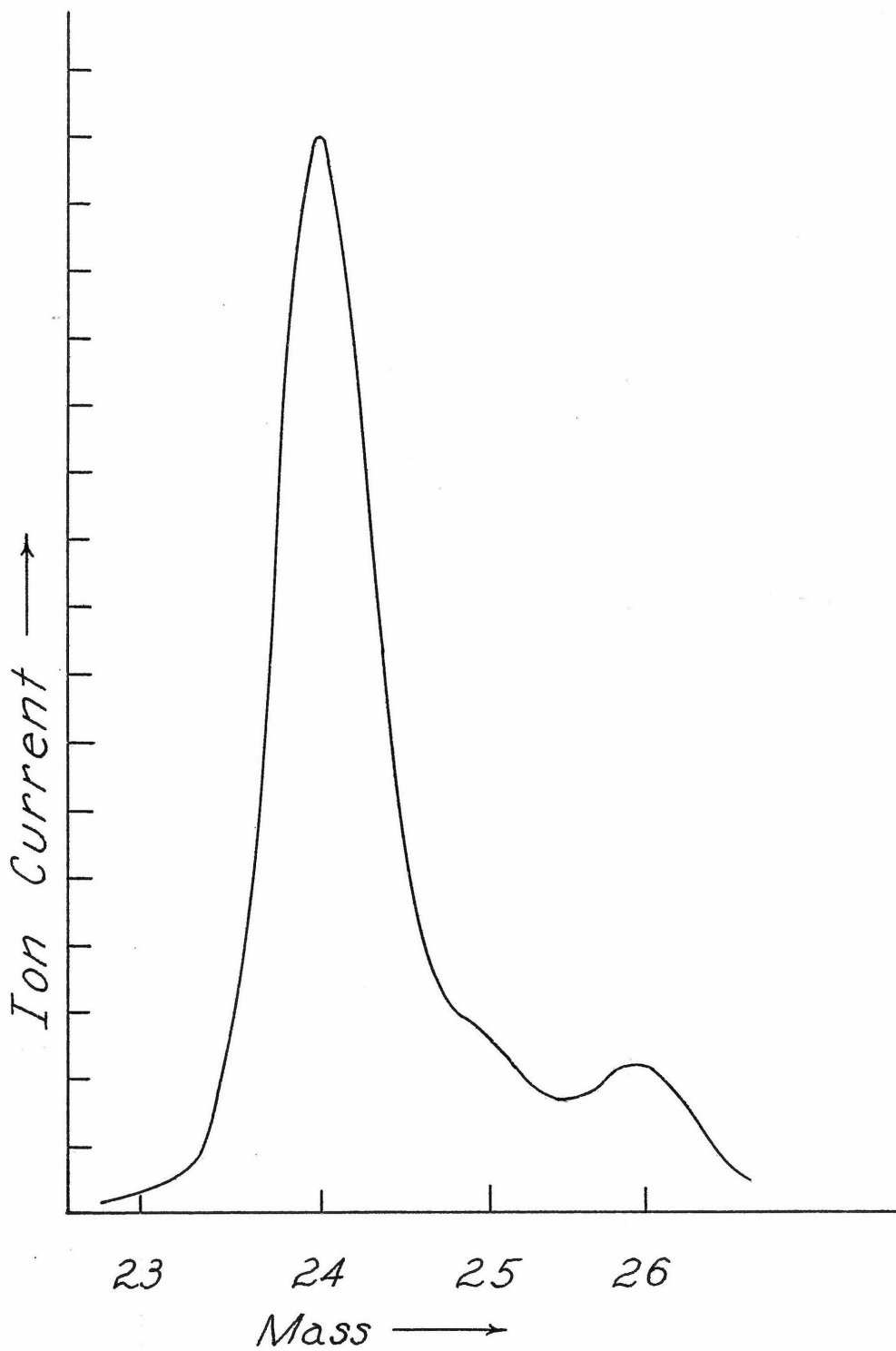


Figure 13

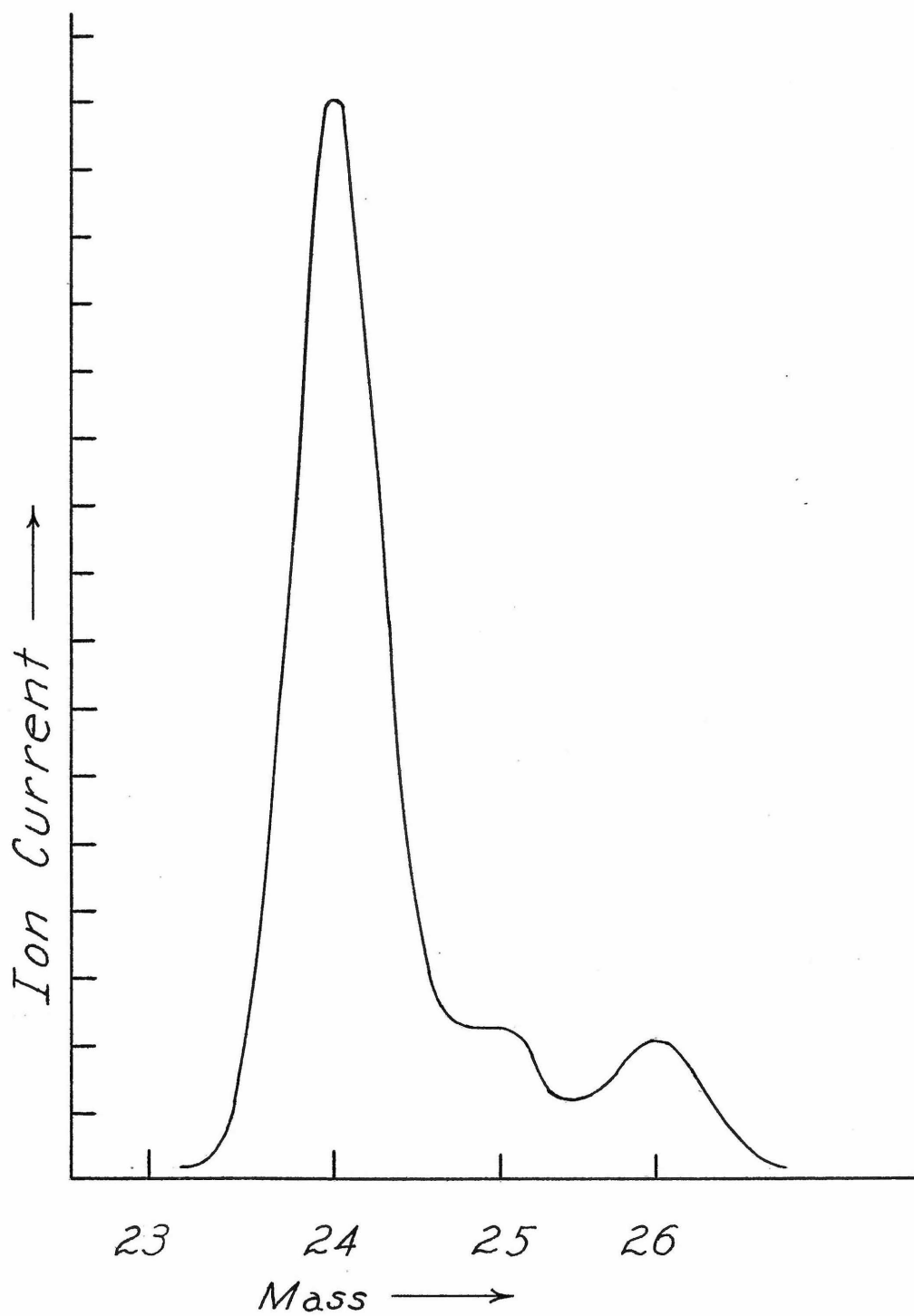


Figure 14

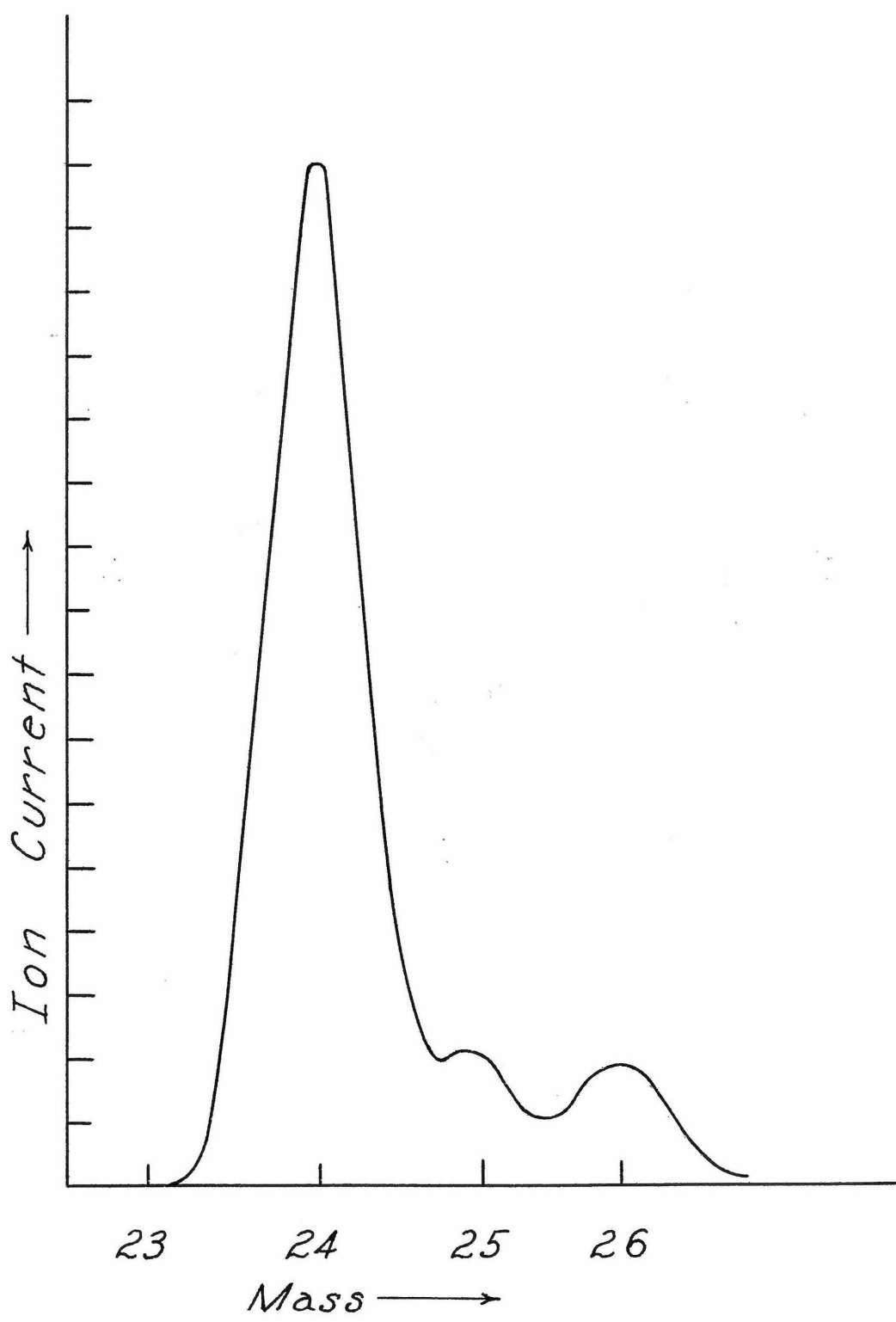


Figure 15

better and the magnetic field was on. Unfortunately, this curve is subject to some doubt since it was discovered later that a protective neon bulb in parallel with the bouncer magnet had an intermittent short in its circuit.

The experimental results led to the following conclusions:

1. All conducting or insulating strips which are in the ion beam should be eliminated, if possible. Those which cannot be eliminated should run parallel to the line source so as to affect the focus rather than the resolution.

2. Filaments parallel to the source can be heated with 60 cycle AC without seriously affecting the resolution.

3. The better the vacuum, the better will be the resolution.

4. Apparently, the magnetic bouncing field affects the resolution to some extent but probably could be used in the collection of the main component.

5. Resolution of the ion current is improved by running the source at lower temperatures and higher voltages (Figure 29.)

Varying the plate voltage from 25v. to 125v. had little effect on the resolution but greatly affected the intensity of the ion current to the collector. The maximum collector current usually occurred when the plate voltage was about 40 volts but this value varied from test to test.

TYPE II SOURCE

The Type I source yielded good resolution. The ion current amounted to 1.5 mils at a pressure of 10^{-5} mm Hg. Using only a single accelerating slit, the current to the collector was 24 microamps. However, it was found that after about 1000 volts were applied between the plate, B, and the accelerator electrode, G, the ion current ceased to increase with the increasing voltage. This could be explained in two ways: (1) the 1000 volts produced a field high enough to draw out all the ions formed. This possibility was discounted by increasing the filament heating current. Neither the electron current nor the positive ion current increased in the ratio expected. (2) The field due to the accelerator voltage was suppressing the electron emission.*

The Type II source (Figure 16) had the filament mounted far down between the plates, B, so that it was electrically shielded from this latter effect. (For approximate penetration of this field see Figure 31.) In addition, the field produced by the high

* The field from the accelerator grid to the filament tended to cancel the field due to the plate voltage, thereby retarding the electron emission.

Source 2

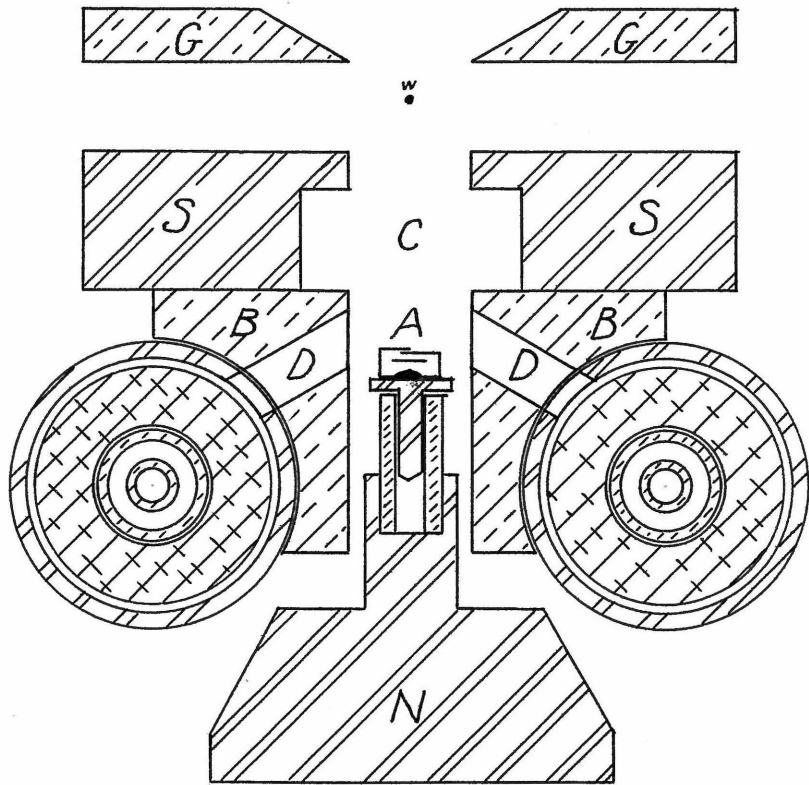


Figure 16

voltage automatically bounced the electrons back toward the filament. It is to be noted that those positive ions which were formed above a certain saddle point were the only ones utilized. This meant that the ions came from a cooler region and hence, on the basis of the Maxwellian thermal distribution, one expected the resolution to be better than in the Type I source. Type II source had the disadvantage that to work efficiently, the bouncer magnetic field had to be used. Figure 16 shows the arrangement of the Type II source tried.

Various vertical positions of the filament were tried. Copper was substituted for iron on the plate, S, while S was moved to the position of G. Various slit widths between the two pieces, S, were tried. Figure 17 shows a representative curve taken with Source II. The maximum current to the collector (aided by a focusing wire) was 40 microamps. However, the resolution was not good. In addition, the life of the source was about four to five hours because the magnesium vapor in the ionization region condensed on the cold iron filament support block, N, piling up beautiful layers of magnesium crystals until it finally shorted against the hot plate, B. This

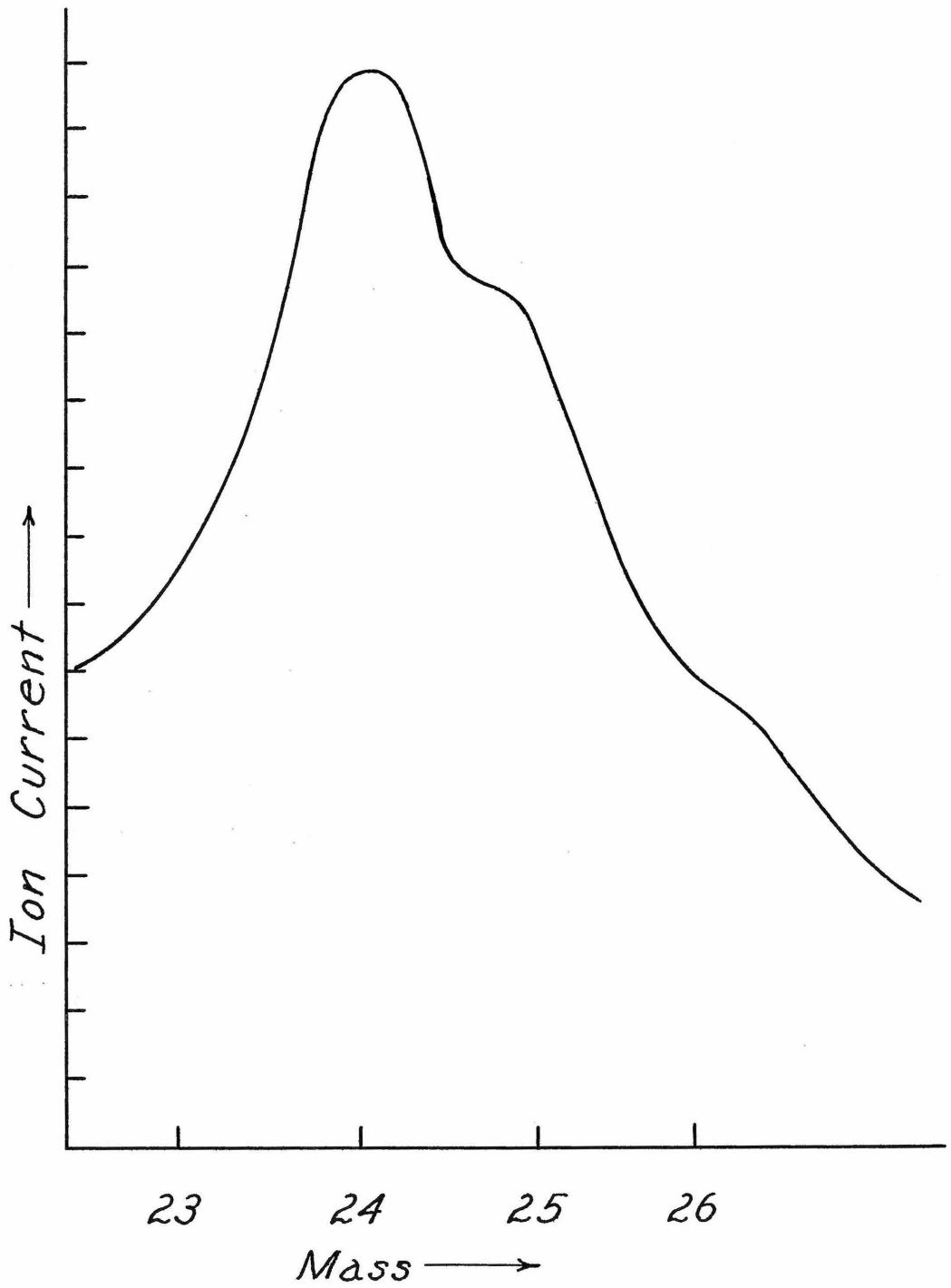


Figure 17

acted like a powerful pump keeping the ionization region at a low pressure, and hence, decreasing the ion current. To counteract this, the magnesium was heated to a higher temperature. This created quite a magnesium gas circulation which tended to destroy the resolution. Type II source had the further disadvantage that the useful ions were produced in a region of low electron density, that is, farther from the filament. In view of the short life of the source, and the poor resolution as shown by the representative experimental curve, the research on Type II source was abandoned. A new source I embodying the constructional advantages of the Type II source was built with the assistance of T. H. Pi. The general plan of the source was similar to that shown in Figure 5 except that copper filament supports were substituted for the pole pieces, S, the latter being placed above the copper. In addition, the width between the filaments was decreased to retard the magnesium losses. The various parts of this source are shown in Figures 18 to 26, inclusive. These are arranged in the order of assembly. The author regrets that he did not have time to test fully this new source. C'est la guerre!



Figure 18 : Source Block

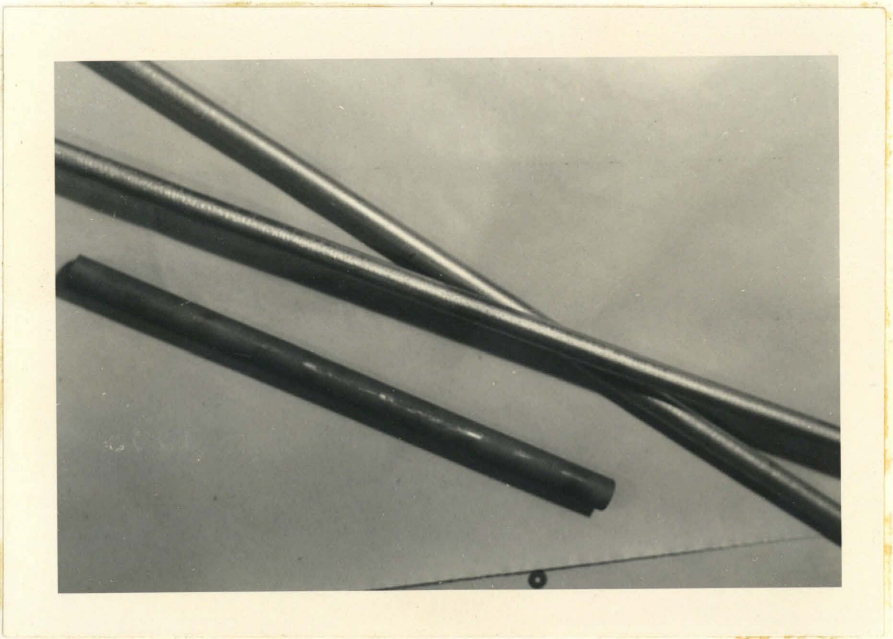


Figure 19 : Magnesium Rods



Figure 20 Plate Assembly

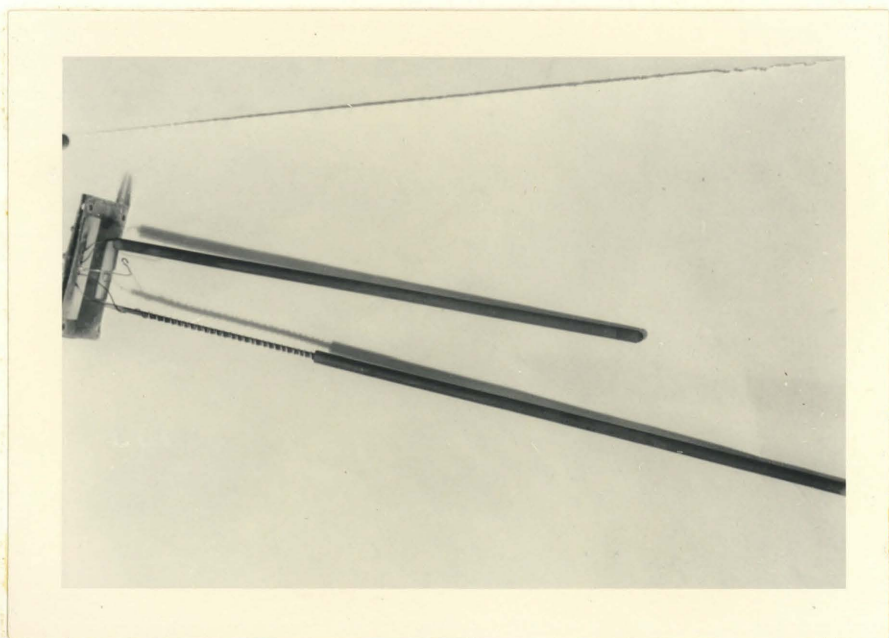


Figure 21 Heaters

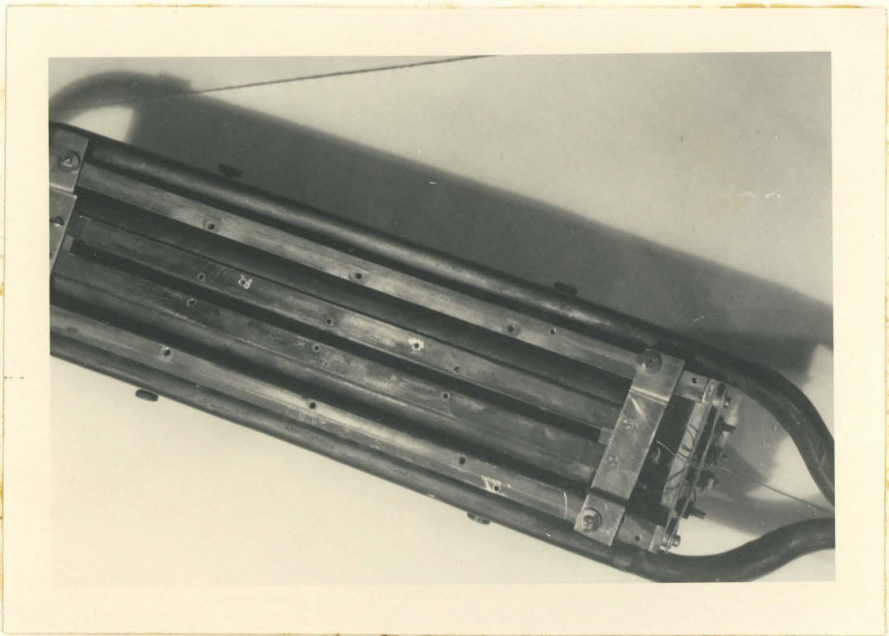


Figure 22 Filament Installation

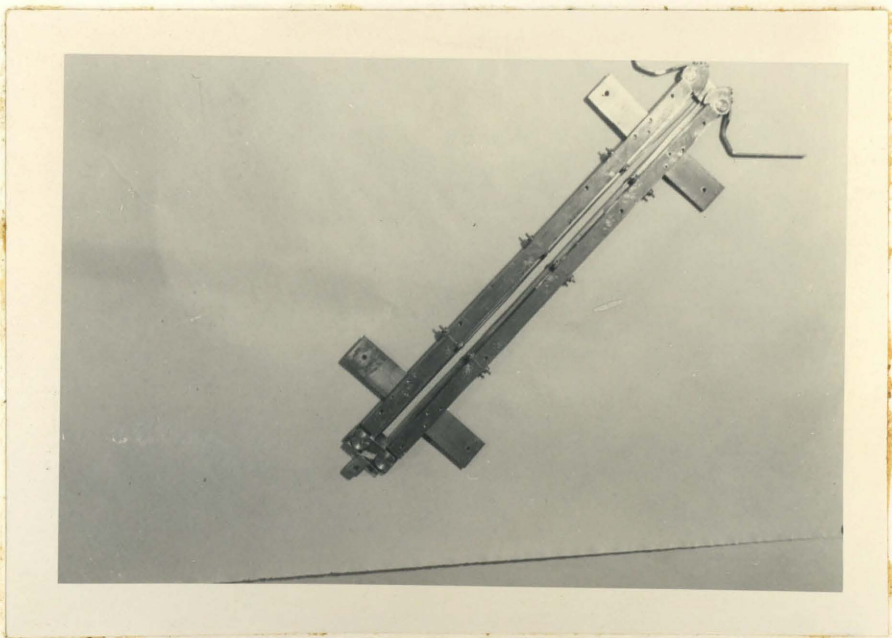


Figure 23 Filament Supports



Figure 24 Filament Supports

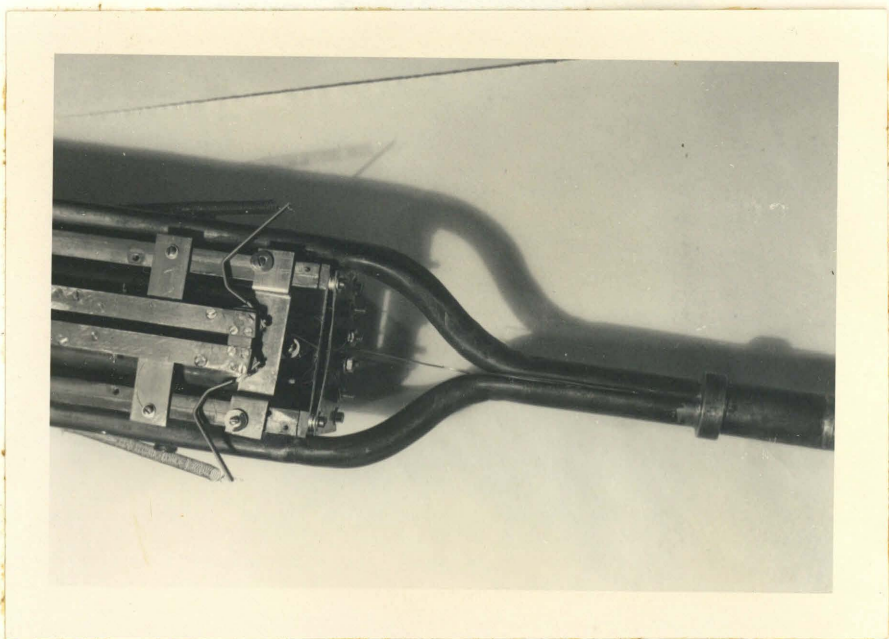


Figure 25 Filaments Installed

Assembled Source

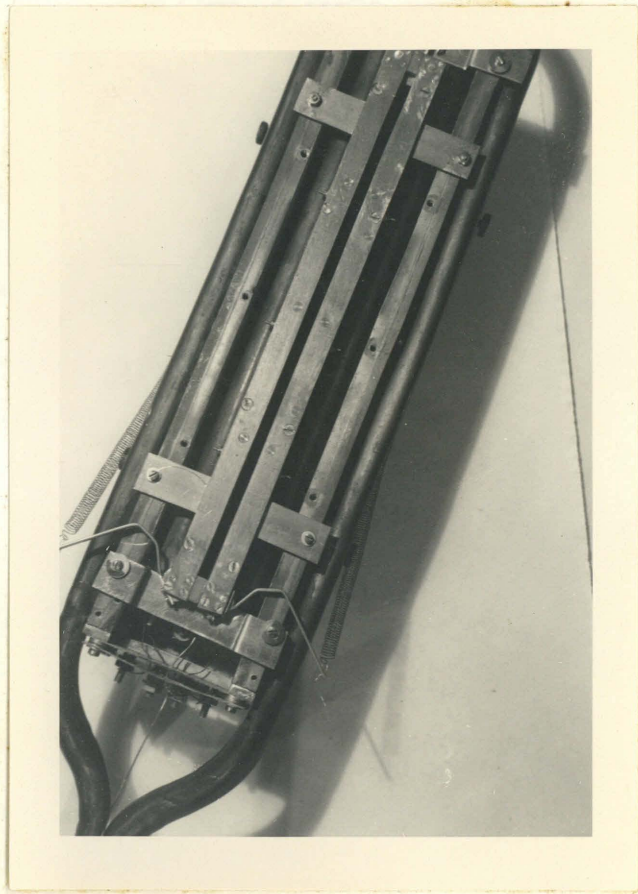


Figure 26

THEORETICAL RESOLUTION

The Maxwell-Boltzmann thermal distribution limits the resolving power of a perfect source. Rumbaugh* had shown that the number of ions emerging from the magnetic field at an angle α is (Figure 27):

$$dN_{\alpha} = CAe^{-\frac{\mathcal{E}}{4k} \left(\frac{\Delta V}{V}\right)^2 \frac{V}{T} \sin^2 \alpha} d\alpha \quad (1)$$

where \mathcal{E} = charge on the ion
 k = Boltzmann constant
 T = absolute temperature
 V = voltage of the center of the peak of the given mass
 ΔV = actual voltage minus V .

However, his method of summing this equation was in error and hence, will be corrected here.

Assume the source emits C ions per unit length. Let X represent the position along the source as shown. Let r represent the radius of curvature of the ion paths. It is clear from the geometry that

$$X = \sqrt{2}r \sin \beta + r = r(\sqrt{2} \sin \beta + 1) \quad (2)$$

$$dX = r\sqrt{2} \cos \beta d\beta. \quad (3)$$

$$\text{But } \alpha = \beta + \pi/4. \quad (4)$$

$$\text{Hence } dX = r(\cos \alpha + \sin \alpha) d\alpha. \quad (5)$$

For the sake of convenience, let us define

$$F = \frac{\mathcal{E}}{4k} \left(\frac{\Delta V}{V}\right)^2 \frac{V}{T} \quad (6)$$

* Ph. D. Thesis, California Institute of Technology.

Spectrometer

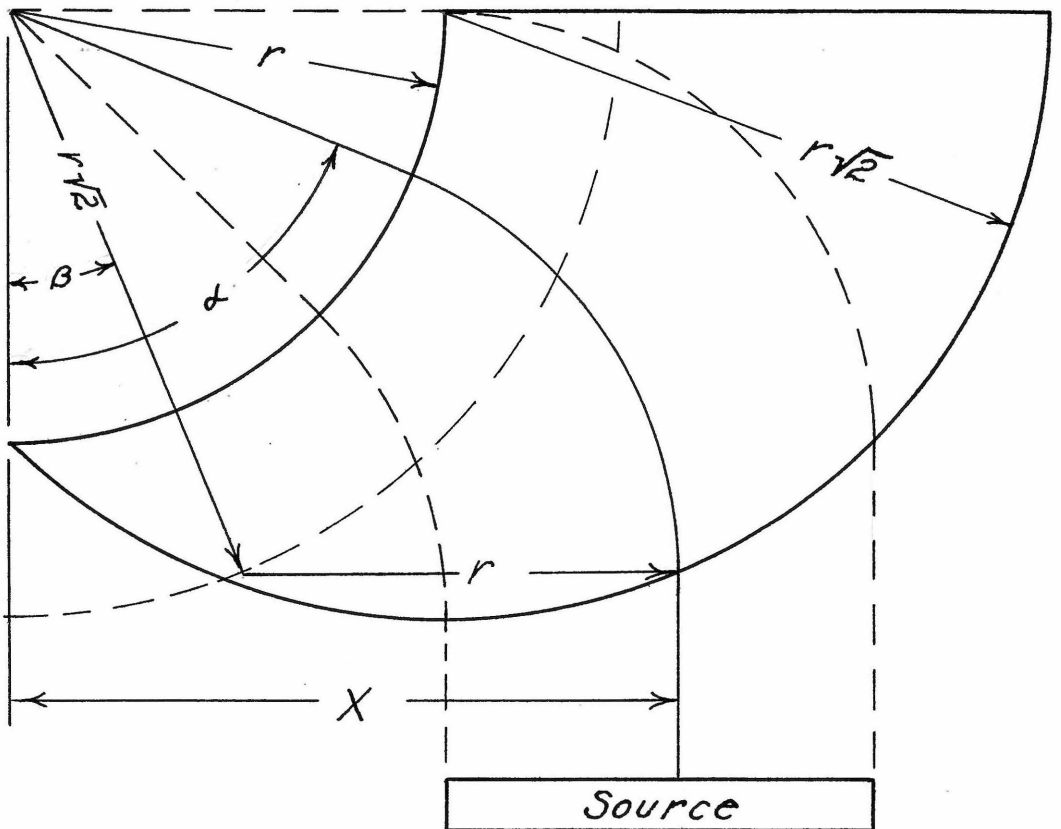


Figure 27

Substituting (5) and (6) into (1) and integrating from $\alpha = \pi/4$ to $\alpha = \pi/2$, we have

$$N = CAR \int_{\pi/4}^{\pi/2} (\cos \alpha + \sin \alpha) e^{-F \sin^2 \alpha} d\alpha \quad (7)$$

But

$$\int_{\pi/4}^{\pi/2} \cos \alpha e^{-F \sin^2 \alpha} d\alpha = \int_{\frac{1}{\sqrt{2}}}^1 e^{-FU^2} du \quad (8)$$

and

$$\int_{\pi/4}^{\pi/2} \sin \alpha e^{-F \sin^2 \alpha} d\alpha = e^{-F} \int_0^{\frac{1}{\sqrt{2}}} e^{FU^2} du \quad (9)$$

$$\therefore I = \frac{N}{CAR} = e^{-F} \int_0^{\frac{1}{\sqrt{2}}} e^{FU^2} du + \int_{\frac{1}{\sqrt{2}}}^1 e^{-FU^2} du \quad (10)$$

The first term in the bracket of (10) has a rapidly converging series and hence is easily summed. The second term of the bracket is the probability integral. This was evaluated by tables. A few values of F with corresponding values of I are given. As a comparison, $e^{-.78F}$ is listed. From this, it is seen that Rumbaugh's equation,

$$N = N_0 e^{-\beta' F} \quad (11)$$

is approximately true. The value of β' is in this case .78.

F	0	.146	.584	1.314	2.336	3.65	5.26	7.16	9.35
I	1	.899	.625	.353	.163	.062	.019	.005	.001+
$e^{-.78F}$	1	.891	.632	.358	.162	.058	.017	.004	.001-

Figure 28 shows a plot of I as a function of F. From this, Figure 29 was computed under the following assumptions:

Isotope	% abundance	Voltage of peak	Abs. Temp.
24	.774	4000	2000 ^o K
25	.115		
26	.111		

Since,

$$\frac{\Delta V}{V} \approx - \frac{\Delta M}{M} \quad (12)$$

curve 29 is approximately equivalent to a source operated at 3500 volts and a temperature of 1750^o K. Figure 29 is to be compared with the experimental curve Figure 15. Combining the approximate equations (11) and (12), we see that the resolution depends exponentially upon the ratio of V/T, thus justifying conclusion (5) of page 30.

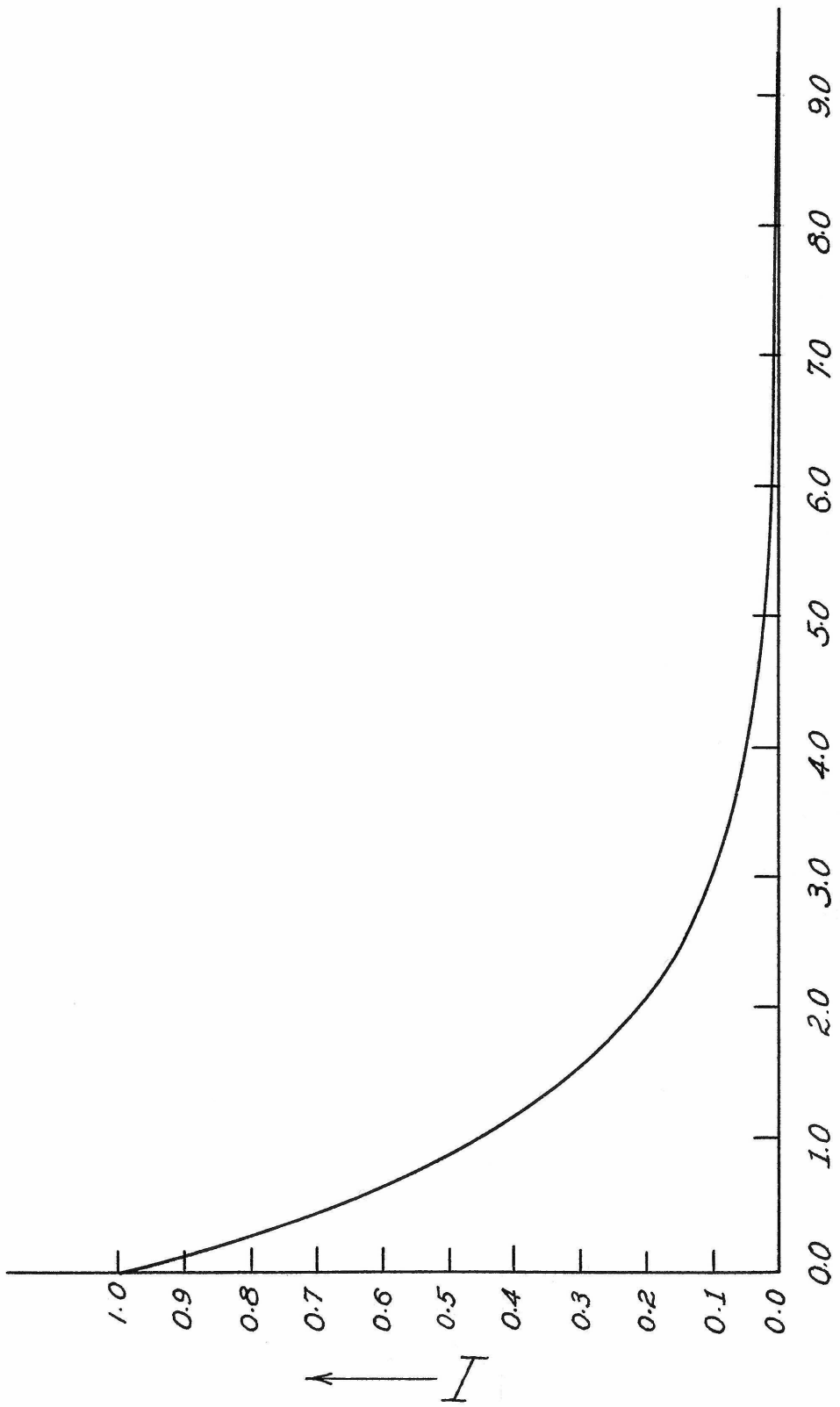


Figure 28

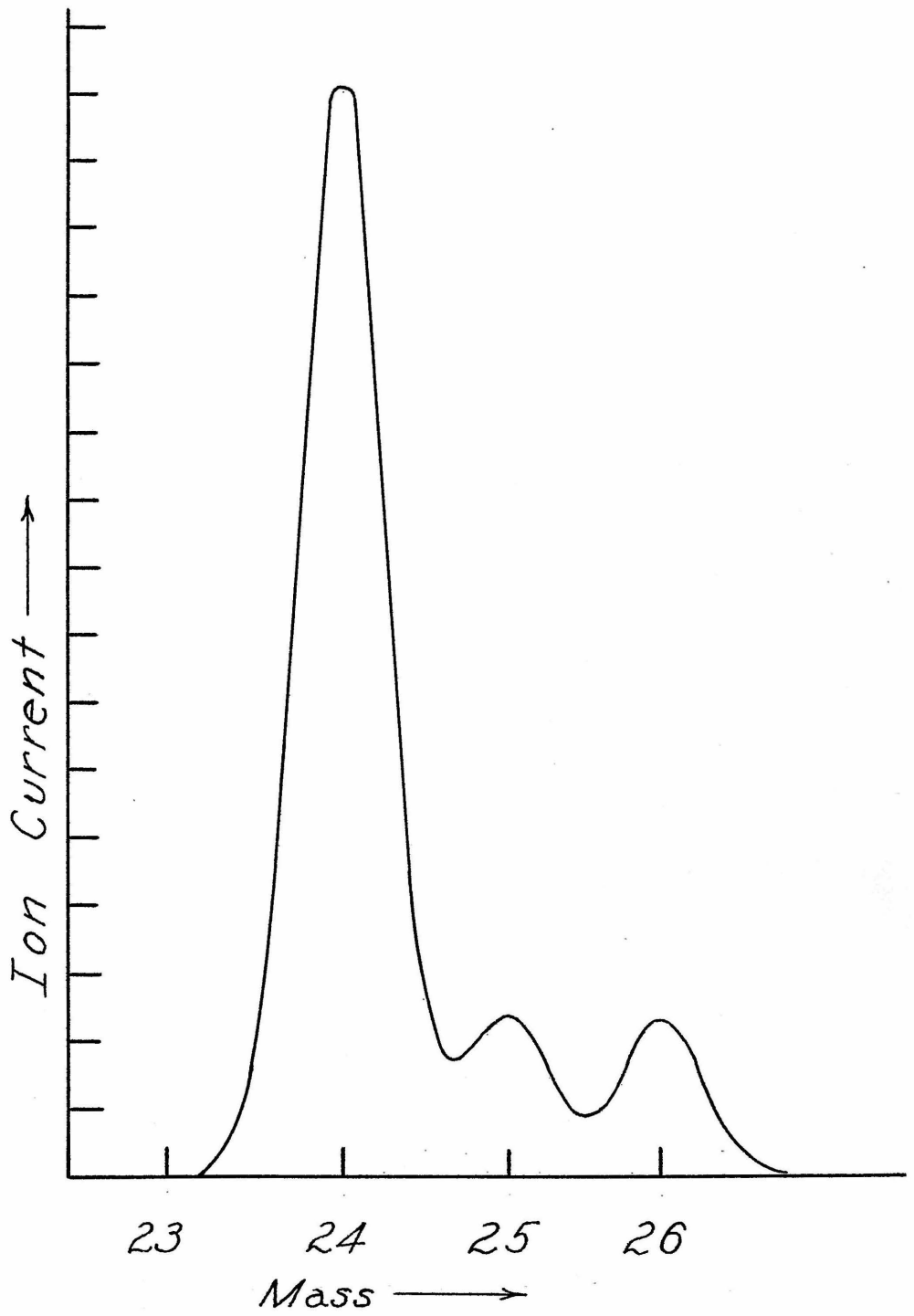


Figure 29

FIELD PENETRATION

Both in the Type I and in the Type II source, it is desirable to know the depth of penetration of the field between S and G into the region C (Figure 16.) We shall approximate the actual arrangement by the slotted pole piece of Figure 30a, which is electrical-ly equivalent to Figure 30b. The Schwartz transformation for Figure 30b is given in "Static and Dynamic Electricity", by Dr. William R. Smythe (page 294) and is

$$Z = \frac{z}{\pi} \left\{ A \sin^{-1} \left[\frac{A}{\sqrt{A^2 + B^2}} \tanh \frac{W}{\delta I} \right] + B \sinh^{-1} \left[\frac{B}{\sqrt{A^2 + B^2}} \sin \frac{W}{\delta I} \right] \right\} \quad (1)$$

where $Z = x + iy$, $W = U + iV$ and I is a constant. In this case, V is the potential function. From Figure 30b and equation (1) we get the following conditions:

$$\text{If } y = 0, \quad V = 0. \quad (2a)$$

$$x = 0, \quad U = 0. \quad (2b)$$

$$y \rightarrow \infty, \quad V \rightarrow V_0. \quad (2c)$$

Putting (2b) and (2c) into (1) and noting that the second term of (1) remains finite for $V = V_0$, we see that

$$V_0 / \delta I = \pi/2. \quad (3)$$

Therefore, if $x = 0$, equation (1) becomes

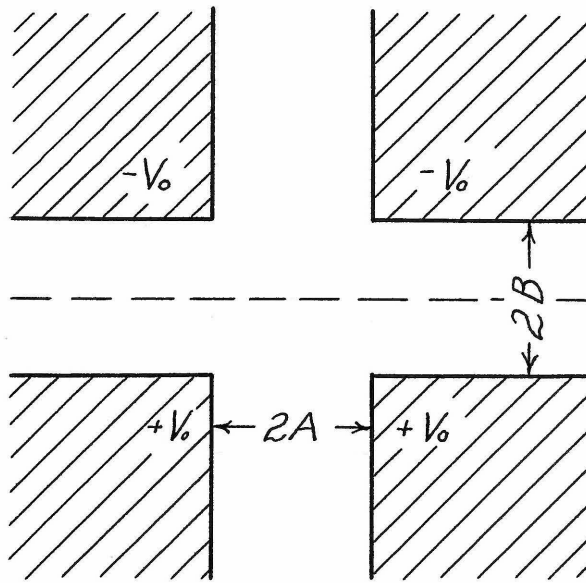


Figure 30a

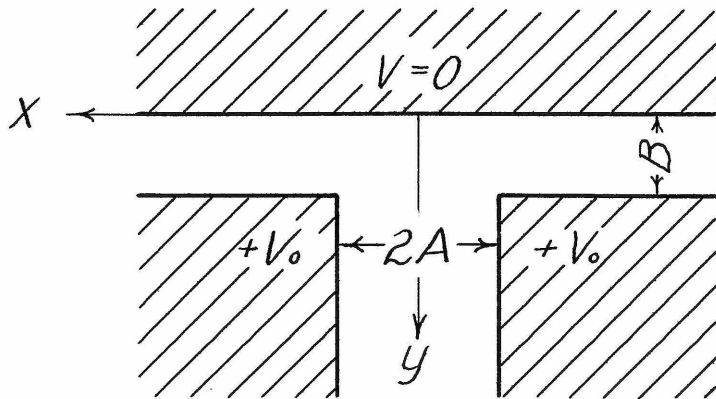


Figure 30b

$$y = \frac{z}{\pi} \left\{ A \sinh^{-1} \left[\frac{A}{\sqrt{A^2 + B^2}} \tan \frac{\pi V}{2V_0} \right] + B \sin^{-1} \left[\frac{B}{\sqrt{A^2 + B^2}} \sin \frac{\pi V}{2V_0} \right] \right\} \quad (4)$$

The field on the $x = 0$ axis is

$$E_y = - \frac{\partial V}{\partial y} \Big|_{x=0} = - \frac{V_0 \cos \frac{\pi V}{2V_0}}{\sqrt{A^2 + B^2 \cos^2 \frac{\pi V}{2V_0}}} \quad (5)$$

For the sake of an approximate calculation, let

$$2A = 5/16", \quad 2B = 5/16", \quad V = 4000 \text{ volts.}$$

$$\text{Hence } A = 5/32", \quad B = 5/32", \quad V_0 = 2000 \text{ volts.}$$

Figure 31 shows the plot of V and $|E_y|$ as a function of the distance y . The position $y = B = 5$ corresponds to the top surface of the Plate, S, of Figure 16.

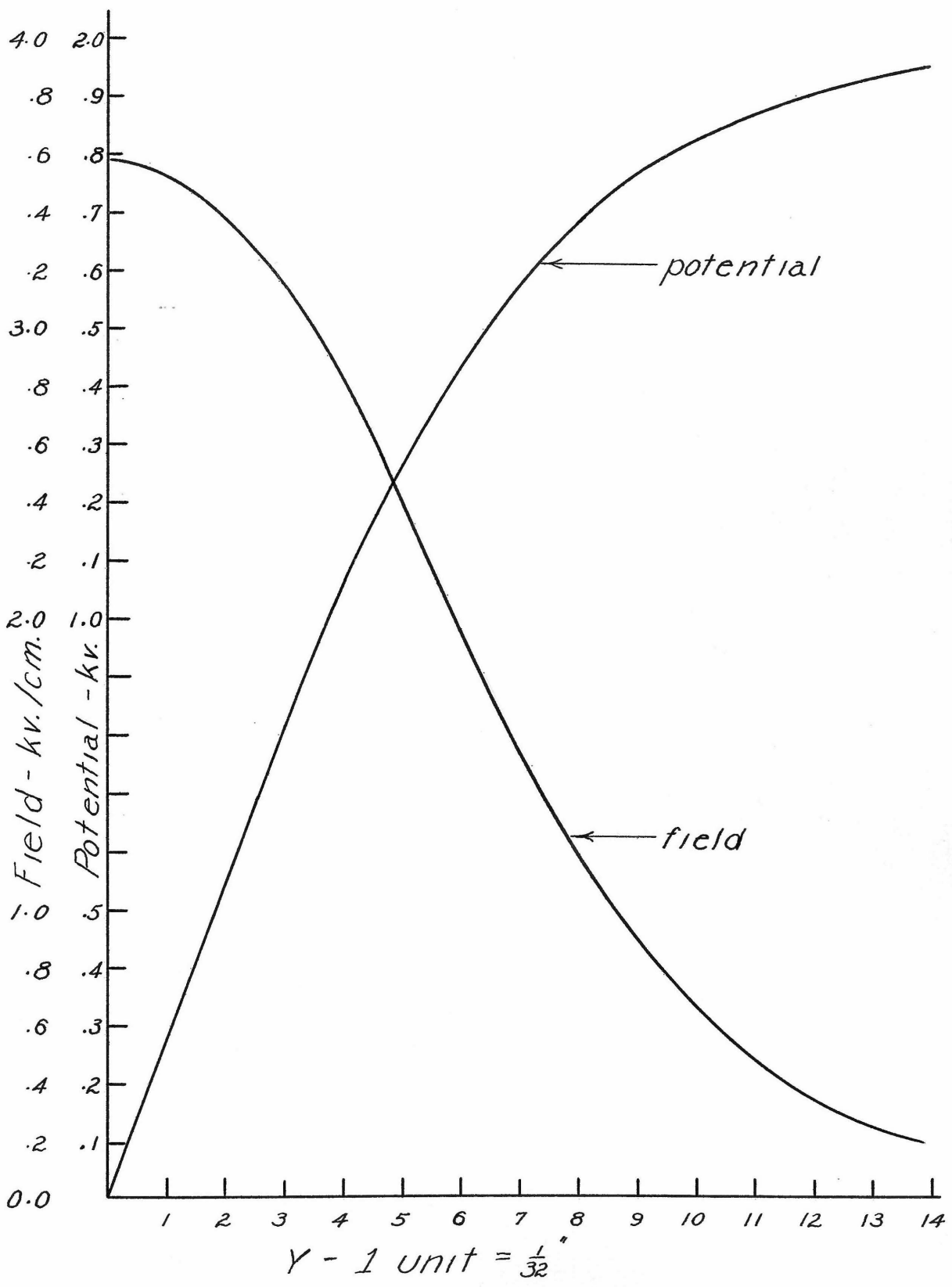


Figure 31

ACKNOWLEDGMENT

The author wishes to express his sincere appreciation to Dr. William R. Smythe, whose constructive suggestions greatly aided the progress of the research.

BIBLIOGRAPHY

1. Aston, "Mass Spectra and Isotopes."
 2. W. R. Smythe, "Static and Dynamic Electricity", McGraw-Hill, 1939.
 3. W. Walker, "Ergebnisse der Exakten Naturwissenschaften, XVIII Band, 1939.
-
1. H. F. Batho and A. J. Dempster, *Astrophys. J.* 75, 34-39 (1932).
 2. H. R. Crane, C.C. Lauritsen and S. Soltar, *Phys. Rev.* 45, 507.
 3. Ann Catherine Davies, *Roy. Soc. Proc.* 155A, 123-124 (May, 1936).
 4. A. J. Dempster, *Phys. Rev.* 18, #15-422 (1921).
 5. A. J. Dempster, *Rev. Sci. Inst.* 7, 46-49 (Jan.'36).
 6. A. Theodore Finkelstein, *Rev. Sci. Inst.* 11, 95.
 7. A. Hemmendinger and W. R. Smythe, *Phys. Rev.* 51, 1052 (1937).
 8. A. Hemmendinger and W. R. Smythe, *Phys. Rev.* 51, 178 (1937).
 9. A. Hemmendinger, Ph.D. Thesis, Calif. Inst. of Tech. (1937).
 10. E. S. Lamar, E. W. Samson, and K.T. Compton, *Phys. Rev.* 48, 887.
 11. E. S. Lamar, W.W. Buechner and K.T. Compton, *Phys. Rev.* 51, 937.
 12. M. Stanley Livingston, M.G. Holloway and C.P. Baker, *Rev. Sci. Inst.* 10, 63.
 13. J.H. Manley and O.S. Duffendack, *Phys. Rev.* 47, 56-61 (1935).
 14. L. H. Rumbaugh, Ph.D. Thesis, Calif. Inst. of Tech. (1932).

15. G. W. Scott, Jr., Phys. Rev 55, 955.
16. Lloyd P. Smith and G. W. Scott, Jr., Phys. Rev. 55, 946 (1939).
17. Lloyd P. Smith and Paul L. Hartman, Journal of Applied Phys. 11, 3, 225.
18. W. R. Smythe, L. H. Rumbaugh and S.S. West, Phys. Rev. 45, 724, 727 (1934).
19. Tuve, Hafstad and Dahl, Phys. Rev. 48, 333.
20. S.S. West, Ph.D. Thesis, Calif. Inst. of Tech. (1934).